Reac Kinet Mech Cat (2011) 104:467–482
DOI 10.1007/s11144-011-0374-4

Liquid-phase furfural hydrogenation employing silica-supported PtSn and PtGe catalysts prepared using surface organometallic chemistry on metals techniques

Andrea B. Merlo · Virginia Vetere · José M. Ramallo-López · Félix G. Requejo · Mónica L. Casella

Received: 5 July 2011 / Accepted: 31 August 2011 / Published online: 17 September 2011

Abstract Platinum–germanium and platinum–tin catalysts supported on silica, containing different amounts of Sn and Ge, were synthesized using the surface organometallic chemistry on metals technique. The catalysts were characterized using transmission electron microscopy, X-ray photoelectron spectra and X-ray absorption near edge structure and extended X-ray absorption fine structure; and were tested in the liquid-phase selective hydrogenation of furfural. The atomic ratio between the two metals resulted the key factor towards the optimization of the activity and selectivity of the bimetallic catalysts. The bimetallic catalysts were more active than the parent Pt/SiO_2 catalyst in the hydrogenation of furfural. These results can be accounted for by considering a new type of active site having an architecture which would favor the hydrogenation of the C=O group is created, allowing an increased activity towards obtaining furfuryl alcohol. All the studied systems allowed to obtain furfuryl alcohol with high selectivity.

Keywords Bimetallic catalysts · PtSn and PtGe · Surface organometallic chemistry · Furfural hydrogenation

A. B. Merlo · V. Vetere · M. L. Casella (✉)
Centro de Investigación y Desarrollo en Ciencias Aplicadas "Dr. Jorge J. Ronco" (CINDECA), Facultad de Ciencias Exactas, Universidad Nacional de La Plata and CCT-La Plata, CONICET calle 47 N° 257, La Plata, Argentina
e-mail: casella@quimica.unlp.edu.ar

J. M. Ramallo-López · F. G. Requejo
Instituto de Investigaciones Fisicoquímicas Teóricas y Aplicadas (INIFTA), Facultad de Ciencias Exactas, Universidad Nacional de La Plata and CCT-La Plata, CONICET Diag. 113 y 64, 1900 La Plata, Argentina

Introduction

Furfural or furfuraldehyde is an important chemical readily accessible from biomass. It seems to be the only unsaturated large-volume organic product prepared from carbohydrate resources and is a key derivative for the production of important nonpetroleum-derived compounds. It is produced from agricultural raw (or waste) materials rich in pentosan polymers (hemicellulose fraction) by acidic degradation. The reaction involves hydrolysis of pentosan into pentoses (mainly xylose), which, under high temperatures (473–523 K) and in the presence of acid catalysts, mainly sulfuric acid, undergo a triple dehydration, giving furfural [1, 2].

There is a large family of primary products that can be obtained from furfural, but 65% of all production becomes furfuryl alcohol [3 and references cited therein]. This compound finds a variety of applications in the chemical industry. Besides being a solvent itself, it is mainly used in the manufacture of resins, as a starting material for the manufacture of tetrahydrofurfuryl alcohol, and it is also an important chemical intermediate for the manufacture of fragrances, vitamin C and lysine [4–6].

Fig. 1 shows the possible hydrogenation products of furfural, arising from the reduction of the C=O group and/or the furan ring. In addition, many other compounds derived from secondary reactions, such as hydrogenolysis of the C–O bond, decarbonylation, hydrogenation and furan ring opening, may appear. The formation of some condensation products of high molecular weight has also been reported [5–7]. Due to the wide variety of compounds available, it is attractive to

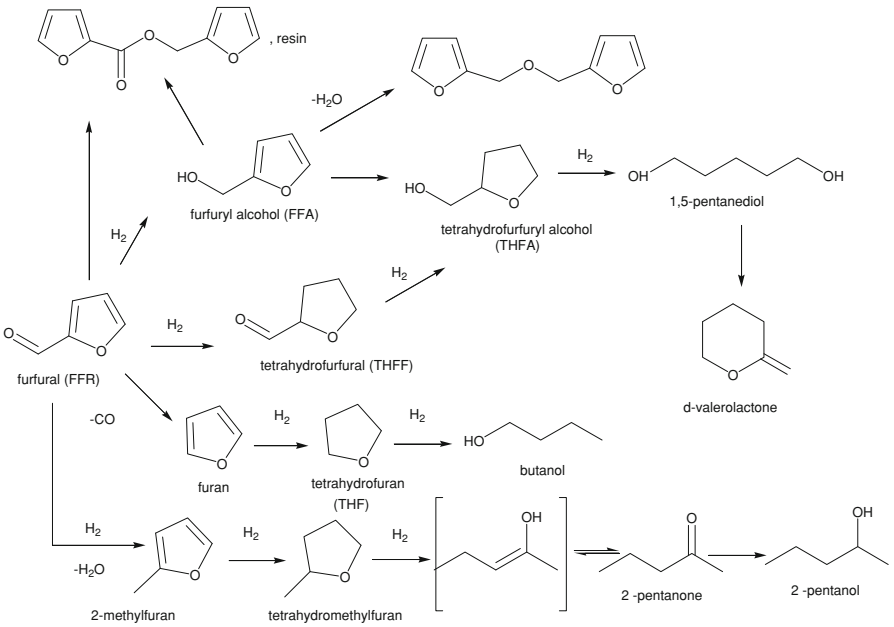

Fig. 1 Reaction scheme for furfural hydrogenation

design systems that are highly selective towards the desired product, furfuryl alcohol.

For over five decades, copper chromite has been the most successful commercial catalyst used. The industrial process employing this catalyst is conducted at high temperature and pressure, which exhibits a moderate activity towards furfuryl alcohol [8–10]. The main drawback of this system is the toxicity of the catalyst, due to the presence of Cr_2O_3, which may have important consequences for the environment [5]. Therefore, the design of active and selective catalytic systems for obtaining the unsaturated alcohol is an issue of interest, which still presents great challenges.

The hydrogenation of furfural in the liquid-phase has been widely studied using catalysts based on Ni, Co, Ru, Pd, and Pt, the latter being much less frequently employed. Sometimes a second metal or a promoter is added to improve the properties of the catalytic systems [5–7, 11, 12]. In this sense, systems based on Ni or Co modified with Cu, Fe, Ce or heteropolyacids have proved to be very successful, reaching 98% selectivity to the unsaturated alcohol, at almost total conversion [13–17].

Previous studies conducted in our research group have shown that the addition of a second, more electropositive metal ($M' = Sn$) to Pt-based systems led to more efficient catalysts in the hydrogenation of many different unsaturated carbonyl compounds [18, 19 and references cited therein]. In this paper, we propose a systematic study using platinum-based silica-supported bimetallic catalysts modified with either $Sn(C_4H_9)_4$ ($SnBu_4$) or $Ge(C_4H_9)_4$ ($GeBu_4$). The objective is to analyze the effect of the addition of the second metal on the activity and selectivity achieved in the liquid-phase hydrogenation of furfural.

Experimental

Catalyst preparation and characterization

The monometallic Pt catalyst was prepared by ion exchange, using SiO_2 (Evonik (previously Degussa) Aerosil 200, 180 $m^2\ g^{-1}$) as support. The silica was previously treated with ammonia solution and, once properly functionalized, it was contacted with an aqueous solution of $[Pt(NH_3)_4]Cl_2$ with an appropriate concentration so as to obtain ca. 1 wt% Pt on the solid. After 24 h of exchange at room temperature, the solid was separated by filtration, washed, dried in an oven at 378 K, and subsequently reduced in H_2 at 773 K for 2 h.

Bimetallic PtSn and PtGe systems were prepared by controlled surface reactions, using techniques derived from the surface organometallic chemistry on metals (SOMC/M) [20 and references cited therein]. According to this procedure, the reduced Pt/SiO_2 catalyst was reacted with a solution of either $SnBu_4$ or $GeBu_4$ in a paraffinic solvent. The reactions were carried out under flowing H_2 at either 363 or 393 K for 4 h, using *n*-heptane or *n*-decane, respectively, as solvent. After the reaction had finished, the liquid phase was separated and the resulting solid was repeatedly washed with *n*-heptane in N_2 flow, and finally treated in H_2 at 773 K for

2 h. The bimetallic catalysts so obtained are designated PtM'_y (M′ = Sn or Ge), where *y* represents the M′/Pt atomic ratio.

The metal contents were determined by atomic absorption (Varian spectra AA 55). The parent monometallic catalyst was studied by temperature-programmed reduction (TPR) (Quantachrome, 25 cm^3 min^{-1}, 5% H_2 in N_2, 10 K min^{-1}), and H_2 and CO chemisorption with a catalyst characterization equipment RXM-100 (Advanced Scientific Designs Inc., USA). The double isotherm method has been used in chemisorption studies.

The content of M′ fixed in each bimetallic catalyst was obtained by chromatographic analysis of the solution containing the organometallic compound, as a function of reaction time, using a Varian CP-3800 gas chromatograph, equipped with a capillary column FactorFour CP8907 (VF-1 ms, 15 m × 0.25 mm i.d., DF = 0.25) and a FID detector. These results were consistent with the values obtained from the analysis of the metal content of bimetallic PtSn catalysts carried out by atomic absorption spectrometry [21].

The size distribution of metal particles was determined by transmission electron microscopy (TEM) using a JEOL 100 CX instrument. The samples were ground and ultrasonically dispersed in distilled water. To estimate the mean particle size, the particles were considered spherical and the second moment of the distribution was employed.

X-ray photoelectron spectra (XPS) were acquired with a multitechnique system (SPECS) equipped with a 100 W Al-K_α X-ray source and a hemispherical electron analyzer PHOIBOS 150, operated in fixed analyzer transmission (FAT) mode. The spectra were collected at an energy pass of 30 eV. The powder samples were pressed to form a disc and mounted onto a manipulator that allowed the transfer from the pretreatment chamber to the analysis chamber. In the pretreatment chamber, the samples were reduced at 673 K for 1 h in flowing H_2. The spectra were recorded once the pressure in the analysis chamber reached a residual pressure of less than 5×10^{-9} mbar. The binding energies were referenced to the C1s line at 284.6 eV. The intensities were estimated by calculating the integral of each peak after subtracting the S-shaped background and fitting the experimental peak to a Lorentzian/Gaussian mix of variable proportion, using the Casa XPS program (CasaSoftware/Casa Software Ltd., UK).

X-ray absorption spectroscopy was measured at the XAFS2 beamline at the Laboratorio Nacional de Luz Sincrotron, Campinas, Brazil. Experiments were performed at ambient temperature in transmission mode using a Si111 monochromator. Samples were sealed in a cell with kapton windows in order to avoid contact with air. Both X-ray absorption near edge structure (XANES) and extended X-ray absorption fine structure (EXAFS) experiments were performed at the Pt L_3 and Ge K edges. Three ion chambers were used as detectors. The sample was positioned between the first and second detectors and a metal foil was placed between the second and the third ones. In order to obtain a better signal-to-noise ratio, two or three spectra were averaged. The raw data were processed using the Athena program. The AUTOBK algorithm was used to fit a smoothly varying background function to the data and to extract the EXAFS oscillation. The Arthemis program, graphical interactive software for EXAFS analysis based on the IFEFFIT library,

was used for the analysis of these data [22]. Theoretical standards used in the data fit were computed using the FEFF6 code [23].

Hydrogenation of furfural

The hydrogenation of furfural was conducted in an autoclave-type reactor (Autoclave Engineers) at 1.0 MPa H_2 pressure, a temperature of 373 K and using 0.25 g of catalyst. Two mL of furfural in 50 mL of 2-propanol as solvent was used in each test (0.5 M).

The evolution of the reaction was followed by gas chromatography in a Varian CP-3800 gas chromatograph equipped with a capillary column CP wax 52 CB (30 m × 0.53 mm) and a FID detector. The reaction products were identified using a GC/MS Shimadzu QP5050 with a capillary column SUPELCO SPB-5^{TM} (30 m, 0.25 mm i.d.).

Results and discussion

The monometallic Pt/SiO_2 catalyst (Pt) was characterized by atomic absorption, TPR, CO and H_2 chemisorption and TEM (Tables 1, 2).

The Pt/SiO_2 catalyst was reduced in H_2 at 773 K for 2 h before performing the chemisorption of H_2 and CO, which yielded similar values (H/Pt = 0.65 and CO/Pt = 0.55). From the chemisorption data, a high dispersion of the metallic phase can be inferred, which is due to the strong interaction between the metal precursor and the support generated by the preparation method (ion exchange). With respect to the TPR test, the diagram presented two major peaks of H_2 consumption: one at 523 K and the other at 723 K, in agreement with the literature information [24]. According to the literature, the low temperature peak can be assigned to the

Table 1 Characterization of the monometallic Pt/SiO_2 catalyst

Catalyst	Pt (wt%)	H/Pt	CO/Pt	d_{TEM} (nm)	TPR (K)	
					Peak 1	Peak 2
Pt/SiO_2	1.0	0.65	0.55	2.0	523	723

Table 2 Main characteristics of Pt, $PtGe_y$ and $PtSn_y$ supported catalysts

Catalyst	M′/Pt(*y*)[a]	H/Pt	d_{TEM} (nm)
Pt/SiO_2	–	0.65	2.0
$PtGe_{0.2}$	0.2	ND	2.1
$PtGe_{0.4}$	0.4	0.15	2.1
$PtGe_{0.6}$	0.6	ND	2.2
$PtSn_{0.2}$	0.2	0.25	1.8
$PtSn_{0.4}$	0.4	0.20	1.8
$PtSn_{0.6}$	0.6	ND	1.9

ND not determined

[a] M′ = Sn, Ge; *y* measured as atomic ratio

presence of Pt(IV) species generated during the calcination pretreatment. The high temperature peak may be assigned to species of the type Pt-$(O–Si\equiv)_y^{n-y}$ (n = 2+ or 4+), formed through the interaction of the metallic precursor and the support [25]. The peaks obtained were broad and presented shoulders, which could be due to the different environment of the ions on the support surface.

The result of TEM characterization for Pt/SiO_2 is presented in Table 1. It can be seen that the mean particle size determined by this technique is 2.0 nm, in agreement with the presence of a considerably dispersed metallic phase. In order to prepare bimetallic catalysts by means of SOMC/M techniques, it is essential that the noble metal present in the parent material possesses small particles and is homogeneously dispersed through the support surface. It is well stated that when the organometallic compound is grafted on a supported metallic particle of a zerovalent metal, it has a higher chemical affinity, and therefore a higher rate of reaction, with the metallic particle than with the oxide support. This kinetic effect renders the field of SOMC/M possible even if the surface area of a metal particle supported on a highly dispersed support does not exceed a few m^2 compared to the surface area of the oxide support. That is the reason why the smaller the particle diameter, the higher the surface area of the particle per unit weight of metal and the more efficient the preparation reaction [26].

A series of modified catalysts, PtM'_y (M′ = Ge, Sn), were obtained by a controlled surface reaction between the monometallic catalyst, previously reduced, and a solution of $SnBu_4$ or $GeBu_4$ in a paraffinic solvent such as *n*-heptane or *n*-decane. This approach, derived from SOMC/M, implies the selective reaction of organometallic compounds of several metals, such as Sn, Ge, Pb, with the surface of transition metals, giving rise to different types of surface structures, such as grafted organometallic fragments, adatoms or bimetallic alloys [27–29].

The following equations describe the two stages of the reaction of organometallic compounds and silica-supported Pt metal particles:

$$Pt/SiO_2 + yM'Bu_4 + \frac{xy}{2}H_2 \rightarrow Pt(M'Bu_{4-x})_y/SiO_2 + xyBuH$$

$$Pt(M'Bu_{4-x})_y/SiO_2 + \frac{(4-x)y}{2}H_2 \rightarrow PtM'_y/SiO_2 + (4-x)yBuH$$

The first stage is carried out at temperatures between 363 and 423 K and leads to a bimetallic system with organic groups anchored onto the surface; the second one occurs between 423 and 773 K, generating the formation of a bimetallic phase, with loss of all the organic fragments. Both supported systems obtained, the organobimetallic ($Pt(M'Bu_{4-x})_y/SiO_2$) and the bimetallic (PtM'_y/SiO_2), have shown interesting catalytic properties in terms of activity, selectivity and stability [30–33].

In order to check the specificity of the reactions that lead to the bimetallic catalysts obtained by SOMC/M methods, blank tests were performed, consisting of the reaction between $M'Bu_4$ and the SiO_2 support. The test was carried out at different temperatures (363, 393 and 423 K) and it was found that the amount of modifier ($SnBu_4$ or $GeBu_4$) that had reacted was less than 1%. This allowed us to conclude that for both tin and germanium, all the promoter had been deposited selectively on the supported metal particles [20]. These results are consistent with

those reported for analogous systems, among others, by Didillon et al. [34] who found, in the case of $RhSn/SiO_2$ catalysts studied by scanning transmission electron microscopy (STEM), that Rh signals were always accompanied by the corresponding Sn signal and that Sn could not be detected in those areas of the support that were not covered with a metallic phase.

Fig. 2 and Table 2 show the influence of increasing amounts of germanium or tin on the mean particle size (measured by TEM) for the studied materials. The metal particle size distribution was in all cases very narrow, with only slight oscillations in d_{TEM} being observed for the bimetallic systems regarding the original Pt/SiO_2 catalyst. These results are in good agreement with the selective addition of Sn over Pt, already reported with other bimetallic systems prepared by SOMC/M techniques [35–37].

Starting from the monometallic catalyst, several bimetallic systems having M′/Pt atomic ratios of 0.2, 0.4 and 0.6 were prepared. The stoichiometry of the bimetallic phase was determined by chromatographic analysis, from the difference between the initial concentration of the organometallic compound and the concentration after the completion of the reaction. The experimental conditions used to obtain the different

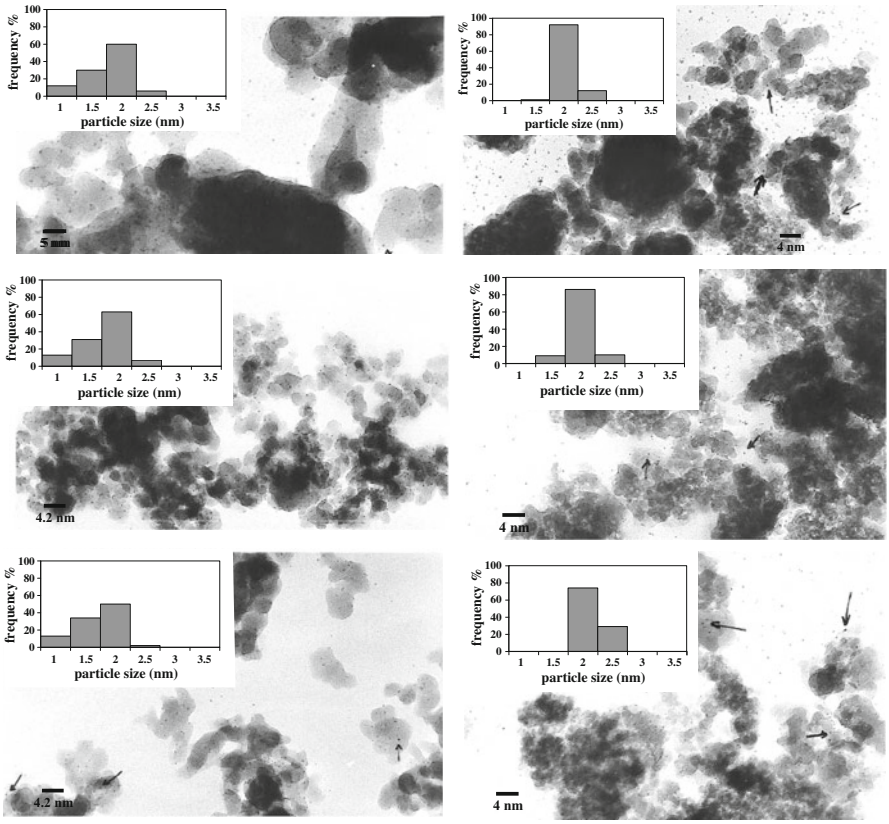

Fig. 2 Particle size distribution for PtSny and PtGey systems on the basis of TEM pictures

M′/Pt atomic ratios studied in this work are listed in Table 3. These results were consistent with the values obtained from the analysis of the metal content of the bimetallic catalysts measured by atomic spectrometry [21]. The reaction temperature and the contact time between the monometallic catalyst and the organometallic compound are two key variables whenever a catalytic system with a certain M′/Pt ratio is to be obtained. From our previous work, we have selected the optimal conditions that allow obtaining bimetallic catalysts with the chosen content of M′ [20]. The results included in Table 3 show that for the lowest Sn concentrations (Sn/Pt = 0.2 and 0.4), all $SnBu_4$ initially present in the impregnation solution reacted on Pt/SiO_2, whereas for achieving the highest Sn/Pt ratio (Sn/Pt = 0.6) a higher temperature was required. In the case of the reaction between $GeBu_4$ and Pt/SiO_2, it is clearly seen that for each of the test temperatures analyzed, higher starting concentration than those used for tin had to be used to obtain the same Ge/Pt ratios. This difference in behavior, as regards their reactivity, can be explained in terms of the substantial difference between M′ and C (M′ = Ge, Sn) bond energies, which have a value of 238 kJ mol^{-1} and 192 kJ mol^{-1} for $GeBu_4$ and $SnBu_4$, respectively [38].

The amounts of tin and germanium fixed on the monometallic catalyst, measured as M′/Pt atomic ratios, as a function of the reaction time for different temperatures, are shown in Fig. 3a, b, respectively. According to the shapes of the curves, the reaction undergoes in two stages, a first one, which is faster, followed by a second one where a plateau in the value of the M′/Pt atomic ratio is reached. As the temperature rises, the initial reaction rate and the plateau value increase. From the analysis of these results, it was confirmed that the selected conditions lead to systems with the M′/Pt desired.

The overall activities of the different catalysts studied are compared considering furfural conversion after 480 min of reaction (Fig. 4). As can be seen from Fig. 4, the presence of the second metal, either Sn or Ge, causes significant changes in the catalytic behavior compared to the monometallic system. In this regard, Sn-modified catalysts were the most active, reaching a conversion close to 100% for the catalysts with an atomic ratio Sn/Pt = 0.2–0.4. A large number of studies can be found in the literature regarding the hydrogenation of carbonyl compounds that

Table 3 Amount of the organometallic compound $M'Bu_4$ (M′ = Sn, Ge) reacted at different temperatures

Catalyst	T (K)	c_i $M'Bu_4$ (mmol L^{-1})[a]	c_f $M'Bu_4$ (mmol L^{-1})[b]
$PtSn_{0.2}$	363	0.41	0
$PtSn_{0.4}$	363	0.90	0
$PtSn_{0.6}$	393	1.46	0.27
$PtGe_{0.2}$	363	0.86	0.38
$PtGe_{0.4}$	393	1.67	0.81
$PtGe_{0.6}$	423	2.34	1.40

[a] c_i = Concentration of the organometallic compound introduced

[b] c_f = Concentration of the organometallic compound remaining unreacted alter 4–6 h

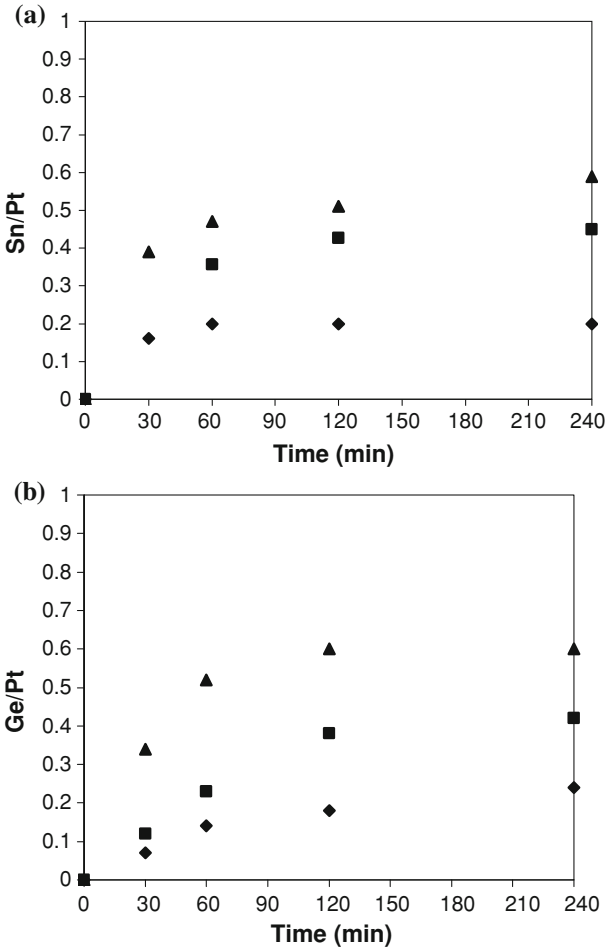

Fig. 3 **a** Amount of tin fixed (measured as Sn/Pt atomic ratio) as a function of time (min): *filled diamond* Sn/Pt = 0.2, *filled square* Sn/Pt = 0.4; *filled up-pointing triangle* Sn/Pt = 0.6. **b** Amount of germanium fixed (measured as Ge/Pt atomic ratio) as a function of time (min): *filled diamond* Ge/Pt = 0.2; *filled square* Ge/Pt = 0.4; *filled up-pointing triangle* Ge/Pt = 0.6

involve a catalyst based on a metal of the group 8, 9, 10 or 11 (mostly of the Pt group), modified with a more electropositive metal to give rise to a bimetallic system. The second metal may be present as an adatom, forming an alloy, in ionic state or partially oxidized. The difference in electronegativity between the two metals may lead to the polarization of the carbonyl bond resulting in high selectivities towards unsaturated alcohols and producing changes in the activity attained. In order to interpret the effect of the presence of a second metal, different mechanisms have been proposed [39 and references cited therein]. The explanation most frequently given for the hydrogenation of many carbonyl compounds suggests that electropositive metals, or oxidized metal species, on the base metal surface act

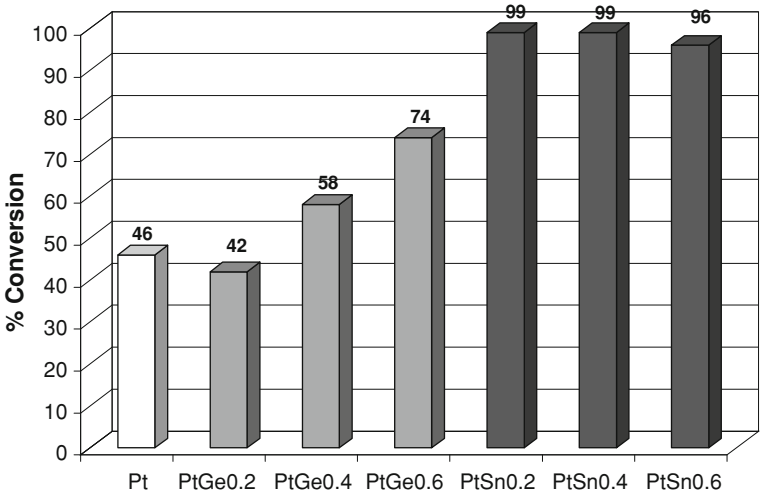

Fig. 4 Furfural hydrogenation, in 2-propanol, at 373 K and $PH_2 = 1.0$ MPa. Conversion at 480 min of reaction

as electrophiles or Lewis acid sites for the adsorption and activation of the C=O bond through a pair of free electrons of the oxygen atom [11].

This explanation is valid for the PtSn systems presented in this paper, since the activation of the C=O group can be assigned to the increase in the electronic density of Pt caused by Sn. Pt and $PtSn_{0.2}$ systems have been characterized by XPS. For both catalysts, the region corresponding to Pt $4f_{7/2}$ showed a single peak, which is characteristic of platinum in the metallic state [40]. The bimetallic sample presented a shift of this peak toward lower BE (71.6 and 71.1 eV for Pt and $PtSn_{0.2}$, respectively). This fact is indicative of the existence of an electronic effect of tin on platinum, in agreement with previous results obtained in studies performed with PtSn catalysts supported on SiO_2 and Al_2O_3, prepared by SOMC/M techniques [41, 42]. The Sn $3d_{5/2}$ spectrum for $PtSn_{0.2}$ presents two bands, one centered at ca. 484 eV that can be ascribed to reduced tin [43], and another one at higher BE (486.3 eV), which is attributed to oxidized tin (Sn(II) and Sn(IV)) [40]. The presence of metallic tin in bimetallic catalysts is an indication of the existence of bimetallic PtSn phases (even alloys), as has been readily assessed by EXAFS analysis performed on systems analogous to the ones employed here [41]. The $PtSn_{0.2}$ catalyst has a Sn(0)/Sn total ratio of 0.55 and a Sn(0)/Pt total ratio of 0.11, which allows us to say that on the catalytic surface two situations occur: (i) dilution of platinum by metallic tin, due to the formation of SnPt phases, and (ii) coverage of the metal particle surface by oxidized tin species. Taking into account the XPS results, the catalytic surface may be depicted by the coexistence of SnPt phases (probably alloys), some segregated metallic platinum and ionic tin located at the platinum-support interface. The presence of these last-mentioned species may be explained in terms of the reactivity of the organotin compound with the metallic surface. It has been deeply studied that when $SnBu_4$ reacts with a metal (M = Pt,

Rh, Ni, etc.) particle, the tin complex migrates from the silica surface to the metal surface where it reacts with the surface hydrogen. The mechanism by which the tin–carbon bond of the grafted organometallic is cleaved by chemisorbed hydrogen is not yet fully understood, but the analogy with mechanisms of molecular chemistry in solution suggests that there is a four-center "transmetallation mechanism" [44, 45]. This pentacoordinated surface intermediate undergoes rapid hydrogenolysis of the Sn–C bonds. The primary surface complex, depending on the metal and the reaction conditions can further lose its ligands by reaction with the surface atoms of the particle to give progressively the dibutyl and monobutyl species and even the totally dealkylated tin species. In this latter case, the tin atom can be considered as an "adatom" on the metal surface. By thermal treatment, this "adatom" may migrate into the first layers of the metal particle, leading to the formation of ionic tin.

Fig. 4 also shows that there is a small decrease in conversion (96%) for the $PtSn_{0.6}$ system. This fact is a clear indication that there is an optimum Sn/Pt ratio, above which the activity decreases due to the blockage of Pt sites, which are active for the hydrogenation, because of the presence of Sn. This result is in agreement with previously published studies on the selective catalytic hydrogenation of cinnamaldehyde with systems analogous to those reported here. The highest reaction rates and TOF (Table 4) values were obtained using a Sn/Pt ratio of 0.2 and 0.4; higher values of Sn/Pt ratios reduced the activity of the system, which may be due to the lower number of active sites for the formation of hydrogen atoms. So, the activity of the bimetallic systems depends on the concentration of tin present in different oxidation states, leading to an optimum Sn/Pt atomic ratio [46].

Ge-modified systems have some interesting differences in their activity compared to the corresponding PtSn systems. The $PtGe_y$ catalysts show higher activity than the monometallic catalyst when the Ge/Pt atomic ratio is 0.4–0.6, with the change in conversion for $PtGe_{0,2}$ being insignificant (Fig. 4; Table 4). The presence of this small amount of Ge decreases the continuous Pt surface and so, the number of active sites. By increasing the amount of Ge added ($PtGe_{0.6}$), a new type of active site, which has higher activity than Pt/SiO_2, would be formed. These results go in the same direction as those reported by Wootsch et al. [47] when studying Ge added to 1% Pt/Al_2O_3 catalyst by controlled surface reaction of Ge $(n\text{-}C_4H_9)_4$ in different amounts. While Ge loading in amounts of 1/12–1/2 monolayers resulted in catalysts with Ge randomly deposited on the surface of Pt, hardly affecting the catalytic behavior as compared with the Ge-free parent catalyst, the addition of 1–2 monolayers of Ge caused a new type of interaction between Pt and Ge.

$PtGe_{0.2}$ and $PtGe_{0.6}$ EXAFS results (Table 5) show that no Pt–Ge bimetallic phase is formed, contrary to what was previously observed in PtSn catalysts [41].

Table 4 TOF obtained for the hydrogenation of furfural using SiO_2 supported Pt, PtSn and PtGe catalysts

Catalyst	Pt/SiO_2	$PtSn_{0.2}$	$PtSn_{0.4}$	$PtSn_{0.6}$	$PtGe_{0.2}$	$PtGe_{0.4}$	$PtGe_{0.6}$
TOF	0.045	0.27	0.22	0.16	0.02	0.06	0.09

Table 5 Parameters obtained from the fits of EXAFS data

	Pair	N	R/Å	σ^2 Å^{-2} ($\times 10^{-3}$)
Pt/SiO_2	Pt-Pt	8.3 ± 1	2.73 ± 0.01	64 ± 2
$PtGe_{0.2}$	Pt-Pt	7.5 ± 0.9	2.75 ± 0.01	67 ± 6
$PtGe_{0.6}$	Pt-Pt	8.5 ± 0.6	2.74 ± 0.01	61 ± 3

N Average coordination number, *R* interatomic distance, σ^2 Debye–Waller factor

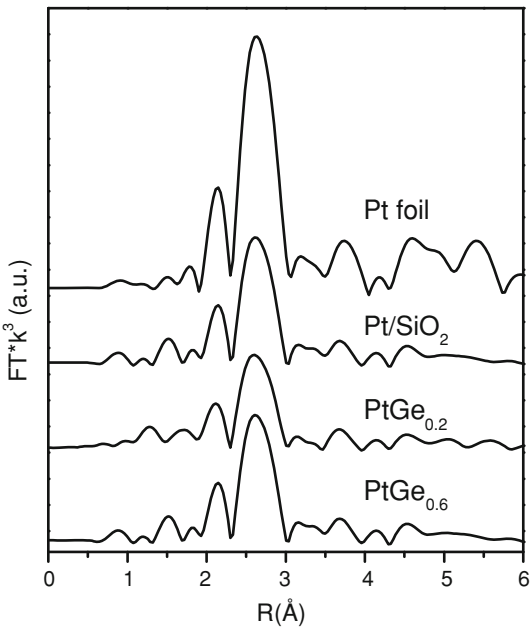

Fig. 5 k^3 Weighted Fourier transform of the extracted EXAFS spectra at the Pt L_3 edge of a foil of Pt, a Pt/SiO_2 catalyst and $PtGe_{0.2}$ and $PtGe_{0.6}$ bimetallic catalysts

EXAFS results at the Pt L_3 edge show that Pt is found forming small metallic particles (Fig. 5). Some interaction between Pt and Ge when germanium is added is also evidenced in the Pt L_3 edge XANES spectra (Fig. 6). The results obtained at the Ge K edge indicate that no metallic phase is observed. Both XANES (not shown here) and EXAFS (Fig. 7) results show Ge forming an oxide phase.

Comparing the behavior of the two promoters employed, the results presented in Fig. 4 indicate that in order to obtain a PtGe catalytic system that leads to a greater activity in the hydrogenation of furfural, a higher Ge/Pt ratio than for the PtSn catalysts is required. In other words, for the same M′/Pt ratio (M′ = Ge, Sn), Sn-modified systems had a greater effect on the activity than the Ge-modified ones. This could be attributed to Sn, as a metal more electropositive than Ge, generate a more favorable electronic effect for the adsorption and activation of C=O. These results agree with those found in the hydrogenation of citral with Ru-based catalysts modified with Pb, Ge and Sn [48].

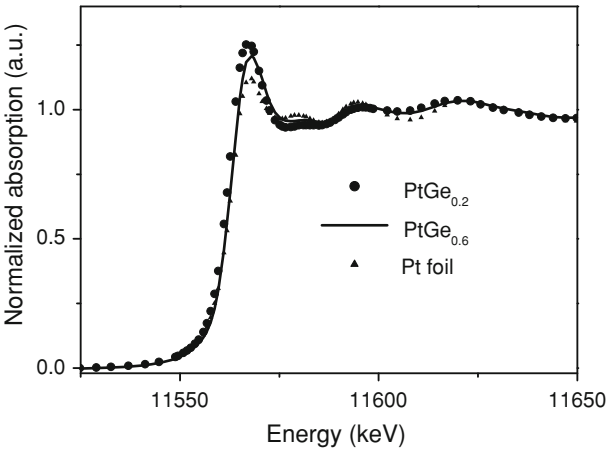

Fig. 6 XANES spectra at the Pt L_3 edge of $PtGe_{0.2}$ and $PtGe_{0.6}$ catalysts compared with that of a foil of metallic Pt

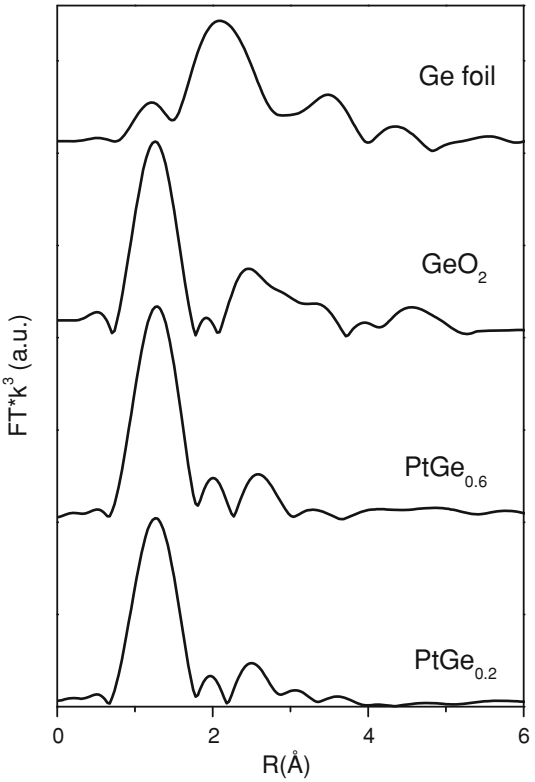

Fig. 7 Fourier transform of the EXAFS spectrum at the Ge *K* edge of reference compounds (Ge foil and GeO_2) and $PtGe_{0.2}$ and $PtGe_{0.6}$ bimetallic catalysts

All the catalysts were highly selective towards the desired product (furfuryl alcohol). Fig. 8 depicts the selectivity obtained after 480 min of reaction for the bimetallic systems studied. These results show that in both systems (PtSn and PtGe),

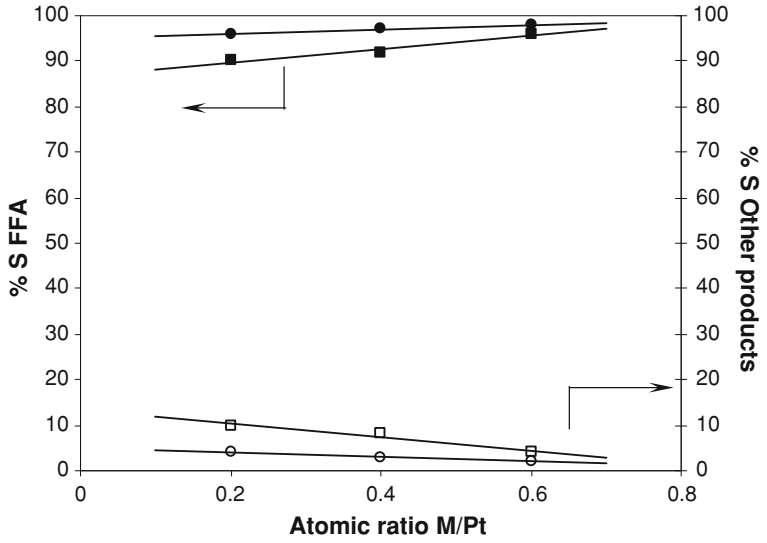

Fig. 8 Dependence of the selectivity to furfutyl alcohol (FFA) (full symbols) and to other hydrogenation products (empty symbols) on the M′/Pt (M′ = Sn, Ge) atomic ratio at 480 min of reaction. *filled* and *open squares* Ge/Pt, *filled* and *open circles* Sn/Pt

the selectivity increases according to the M′ content fixed, this effect being more noticeable in the $PtGe_y$ systems. The second metal would act as a promoter for the adsorption of the C=O group, which is otherwise polarized and susceptible to being reduced by hydrogen chemisorbed on the Pt atoms. The $PtGe_y$ systems were somewhat less selective than the $PtSn_y$ catalysts, in agreement with the results obtained by other authors in the hydrogenation of carbonyl compounds [49].

Finally, it is interesting to note that, for all catalysts used, a minor product of the reaction between furfuryl alcohol and the reaction solvent (propan-2-ol), 2-isopropoxymethylfuran, has been obtained. In a recent study conducted by our research group, we showed that although the use of solvents that do not contain an alcohol function prevents the formation of this ether, the catalyst activity decreases dramatically, proving that propan-2-ol is a suitable solvent for this reaction [18]. On the other hand, undesirable reaction products such as hydrogenolysis or decarbonylation have not been observed.

Conclusions

The main conclusions of this work are summarized below:

- Bimetallic catalysts have been obtained by a controlled surface reaction between a Pt/SiO_2 catalyst and organometallic compounds in solution ($GeBu_4$ and $SnBu_4$). The reaction conditions had to be carefully studied to obtain different M′/Pt atomic ratios (M′ = Ge, Sn).

- All the catalysts were highly selective towards the desired product (furfuryl alcohol). In bimetallic systems, the selectivity increases according to the M′ content fixed, this effect being more noticeable in the $PtGe_y$ systems.
- All the systems were active in the liquid-phase hydrogenation of furfural. The bimetallic catalysts were more active than the parent Pt/SiO_2 catalyst, with the only exception of $PtGe_{0.2}$ catalyst. These results can be accounted for by considering a new type of active site having an architecture which would favor the hydrogenation of the C=O group is created, allowing to increased activity towards obtaining furfuryl alcohol.
- Bimetallic catalysts were highly selective towards the desired product (furfuryl alcohol). These results can be accounted for by considering that in spite of dilution effect of active sites on platinum, the architecture of the resulting active sites favors the hydrogenation of the C=O group, allowing the preferential formation of furfuryl alcohol.
- The M′/Pt atomic ratio is key when the activity and selectivity of the bimetallic systems studied is to be optimized.

Acknowledgments This work has been sponsored by CONICET (Argentina) (PIP 06527, PIP 112-200801-03079), ANPCyT (Argentina) (PICT 25827, PICT 00038), Universidad Nacional de La Plata, Argentina and LNLS (Projects D04B-XAFS1-3525 and D04B-XAFS1-4082), Brazil.

References

1. Zeitsch KJ (2000) The chemistry and technology of furfural and its many by-products, 1st edn. Vol 13. Elsevier, Amsterdam
2. Kim YC, Lee HS (2001) J Ind Eng Chem 7:424–429
3. Corma A, Iborra S, Velty A (2007) Chem Rev 107:2411–2502
4. Nagaraja BM, Kumar VS, Shasikala V, Padmasri AH, Sreedhar B, Raju BD, Rao KSR (2003) Catal Comm 4:287–293
5. Nagaraja BM, Padmasri AH, Raju BD, Rao KSR (2007) J Mol Catal A 265:90–97
6. Kijenski J, Winiarek P, Paryjczak T, Lewicki A, Mikołajska A (2002) Appl Catal A 233:171–182
7. Zheng HY, Zhua YL, Teng BT, Bai ZQ, Zhang CH, Xiang HW, Li YW (2006) J Mol Catal 246:18–23
8. Wu J, Shen Y, Liu Ch, Wang H, Geng C, Zhang Z (2005) Catal Comm 6:633–637
9. Rao R, Dandekar A, Baker RTK, Vannice MA (1997) J Catal 171:406–419
10. Frainier LJ, Fineberg H (1981) US Patent 4,302,397
11. Mäki-Arvela P, Hájek J, Salmi T, Murzin DY (2005) Appl Catal A 292:1–49
12. Vaidya PD, Mahajani VV (2003) Ind Eng Chem Res 42:3881–3885
13. Merat N, Godawa C, Gaset A (1990) J Chem Technol Biotechnol 48:145–159
14. Li H, Luo H, Zhuang L, Dai W, Qiao M (2003) J Mol Catal A 203:267–275
15. Chen X, Li H, Luo H, Qiao M (2002) Appl Catal A 233:13–20
16. Li H, Zhang S, Luo H (2004) Mater Lett 58:2741–2746
17. Baijun L, Lianhai L, Bingchun W, Tianxi C, Iwatani K (1998) Appl Catal A 171:117–122
18. Merlo AB, Vetere V, Ruggera JF, Casella ML (2009) Catal Comm 10:1665–1669
19. Vetere V, Merlo AB, Ruggera JF, Casella ML (2010) J Braz Chem Soc 21(5):914–920
20. Ferretti OA, Casella ML (2009) In: Basset JM, Psaro R, Roberto D, Ugo R (eds) Modern surface organometallic chemistry. Wiley–VCH, Weinheim, 239–291
21. Vetere V (2007) PhD Thesis, University of La Plata, Argentina
22. Ravel B, Newville M (2005) J Synchrotron Radiat 12:537–541
23. Zabinsky SI, Rehr JJ, Ankudinov A, Albers RC, Eller MJ (1995) Phys Rev B Condens Matter 52:2995–3009

24. Merlen E, Beccat P, Bertolini JC, Delichere F, Zanier N, Didillon B (1996) J Catal 159:178–188
25. Ho LW, Hwang CP, Lee JF, Wang I, Yeh CT (1998) J Mol Catal A 136:293–299
26. Basset JM, Baudouin A, Bayard F, Candy JP, Copéret C, De Mallmann A, Godard G, Kuntz E, Lefebvre F, Lucas C, Norsic S, Pelzer K, Quadrelli A, Santini C, Soulivong D, Stoffelbach F, Taoufik M, Thieuleux C, Thivolle-Cazat J, Veyre L (2009) In: Basset JM, Psaro R, Roberto D, Ugo R (eds) Modern surface organometallic chemistry. Wiley–VCH, Weinheim, 23–74
27. Didillon B, Houtman C, Shay T, Candy JP, Basset JM (1993) J Am Chem Soc 115:9380–9388
28. Margitfalvi JL, Borbáth I, Tfirst E, Tompos A (1998) Catal Today 43:29–49
29. Santori GF, Casella ML, Siri GJ, Adúriz HR, Ferretti OA (2000) Appl Catal A 197:141–149
30. Didillon B, Candy JP, Le Peletier F, Ferretti OA, Basset JM (1993) Stud Surf Sci Catal 78:147–154
31. Humblot F, Cordonnier MA, Santini C, Didillon B, Candy JP, Basset JM (1997) Stud Surf Sci Catal 108:289–296
32. Vetere V, Faraoni MB, Santori GF, Podestá J, Casella ML, Ferretti OA (2004) J Catal 226(2): 457–468
33. Casella ML, Santori GF, Moglioni A, Vetere V, Ruggera JF, Iglesias GM, Ferretti OA (2007) Appl Catal A 318:1–8
34. Didillon B, Candy JP, Mansour AE, Houtmann C, Basset JM (1992) J Mol Catal 74(1–3):43–49
35. Candy JP, El Mansour A, Ferretti OA, Mabilon G, Bournonville JP, Basset JM, Martino G (1988) J Catal 112:201–209
36. Ferretti OA, Bournonville JP, Mabilon G, Martino G, Candy JP, Basset JM (1991) J Mol Catal 67:283–294
37. Ferretti OA, Lucas C, Candy JP, Basset JM, Didillon B, Peltier FL (1995) J Mol Catal A 103: 125–132
38. Pruchnik FP (1990) Organometallic chemistry of the transition elements. Plenum Press, New York
39. Gallezot P, Richard D (1998) Catal Rev Sci Eng 40:81–126
40. Wagner CD (1989) NIST X-ray photoelectron spectroscopy database. Gaithersburg
41. Ramallo-Lopez JM, Santori GF, Giovanetti GFL, Casella ML, Ferretti OA, Requejo FG (2003) J Phy Chem B 107:11441–11451
42. Siri GJ, Ramallo-López JM, Casella ML, Fierro JLG, Requejo FG, Ferretti OA (2005) Appl Catal A 278:239–249
43. Rodriguez JA, Jirsak T, Chaturvedi S, Hrbek J (1998) J Am Chem Soc 120:11149–11157
44. Taoufik M, Cordonnier MA, Santini CC, Basset JM, Candy JP (2004) New J Chem 28:1531–1537
45. Jubert AH, Michelini MC, Estiu GL, Ferretti OA (1997) Catal Lett 46:241–247
46. Merlo AB, Machado BF, Vetere V, Faria JL, Casella ML (2010) Appl Catal A 383:43–49
47. Wootsch A, Paál Z, Győrffy N, Ello S, Boghian I, Leverd J, Pirault-Roy L (2006) J Catal 238:67–78
48. Neri G, Mercadante L, Milone C, Pietropaolo R, Galvagno S (1996) J Mol Catal A 108:41–50
49. Vilella IMJ, de Miguel SR, Scelza AO (2008) J Mol Catal A 284:161–171